J Fluoresc (2011) 21:521–529
DOI 10.1007/s10895-010-0738-6

ORIGINAL PAPER

Unusual Excited State Characteristics of 6-aminobenzothiazole with β-cyclodextrin

Rajamohan Rajaram · Kothai Nayaki Sundararajalu · Swaminathan Meenakshisundaram

Received: 10 July 2010 / Accepted: 28 September 2010 / Published online: 14 October 2010

Abstract The interaction between 6-aminobenzothiazole (6ABT) and β-cyclodextrin (β-CDx) has been investigated in solution and solid state. The stoichiometry and binding constants of the complex between 6ABT and β-CDx in solution have been determined by steady state and time-resolved fluorescence spectroscopy. Fluorescence intensity of neutral form decreases during complexation which is contrary to the usual observation. This is explained by hydrogen bonding interaction between lone pair of nitrogen with OH groups of β-CDx. The FT-IR spectral study and SEM images of solid complex confirmed the formation of inclusion complex. Excited state acidity constants for 6ABT have been determined in aqueous and β-CDx medium and discussed.

Keywords 6-aminobenzothiazole · Inclusion complex · β-cyclodextrin · Binding constants · Acidity constants

Introduction

Molecular recognition in chemistry and biology is of current interest in supramolecular chemistry and can be characterised quantitatively and qualitatively by fluorescence due to alteration of the photophysical processes induced by environmental stimuli. Cyclodextrins are one of the most important host molecules in supramolecular chemistry. Cyclodextrins have toroidal shape with an internal hydrophobic surface and an external hydrophilic surface [1–6]. These naturally occurring cyclodextrins are well known for the formation of stable host-guest inclusion complexes. The chemical reactivity and the spectroscopic properties of the guest molecules are modified as a result of the inclusion.

Inclusion complexation depends on the size, shape and hydrophobicity of the guest molecule, thus mimicking biochemical selectively, which is due to the orientation of the substrate by complex formation. The "goodness of fit" between host and guest is the most important factor in complexation [1]. Encapsulation and photochemical investigation in such organized assemblies is an extremely active area of research in the wide of supramolecular chemistry for both fundamental studies and practical purposes [7–10].

Several driving forces have been proposed for the inclusion of β-CDx with substrate including hydrogen bonding, van der Walls forces, hydrophobic interaction and the release of 'high energy water' molecules from the cavity [11, 12]. As a result of complex formation the characteristic properties of the included substance, such as solubility, chemical reactivity and spectral properties will be changed. β-cyclodextrin is the favourite cyclodextrin for the encapsulation of most of the organic fluorophores due to its cavity size.

The supramolecular complex between amino-substituted benzothiazole and substituted phenethylamide through the donor-acceptor complex was studied [13]. The amino substituted benzothiazoles were used in the synthesis of Schiff bases [14]. The formation of 6-aminobenzothiazole inclusion complex with β-CDx may give a way for its synthetic utility. Earlier we reported the inclusion complex-

R. Rajaram
Department of Chemistry, SKP Institute of Technology, Tiruvannamalai 606 611, India

S. Meenakshisundaram (✉)
Department of Chemistry, Annamalai University, Annamalainagar 608 002, India
e-mail: chemsam50@gmail.com

K. N. Sundararajalu
Chemistry Section, FEAT, Annamalai University, Annamalainagar 608 002, India

Table 1 Absorption and fluorescence maxima of 6-aminobenzothiazole (6ABT) at different concentrations of β-CDx

Concentration of β-CDx	pH 6.9				pH 1.1			
	λ_{abs} (Abs)	λ_{abs} (Abs)	λ_{abs} (Abs)	λ_{emi} (nm)	λ_{abs} (Abs)	λ_{abs} (Abs)	λ_{abs} (Abs)	λ_{emi} (nm)
0	282.0 (0.098)	244.2 (0.098)	223.8 (0.203)	349.0 426.0	282.0 (0.070)	249.0 (0.110)	233.0 (0.139)	348.0 420.0
2×10^{-3}	281.4 (0.125)	244.2 (0.124)	224.8 (0.234)	349.0 425.0	281.6 (0.093)	249.2 (0.139)	233.0 (0.165)	348.0 419.0
4×10^{-3}	280.4 (0.139)	243.6 (0.153)	224.4 (0.235)	349.0 425.0	281.6 (0.095)	249.4 (0.143)	233.2 (0.168)	348.0 416.0
6×10^{-3}	280.2 (0.191)	242.6 (0.232)	225.8 (0.312)	349.0 424.0	280.8 (0.107)	249.6 (0.157)	232.2 (0.180)	347.0 414.0
8×10^{-3}	280.4 (0.199)	242.4 (0.244)	225.0 (0.333)	349.0 423.0	280.6 (0.129)	250.2 (0.186)	231.0 (0.219)	347.0 415.0
10×10^{-3}	279.8 (0.235)	242.4 (0.286)	225.2 (0.393)	349.0 420.0	280.0 (0.143)	250.0 (0.195)	229.8 (0.231)	348.0 418.0
12×10^{-3}	279.6 (0.271)	242.2 (0.331)	225.6 (0.443)	349.0 423.0	279.4 (0.158)	250.2 (0.220)	229.4 (0.256)	347.0 417.0

ation of 2-amino-6-nitrobenzothiazole [15], amino substituted benzothiazole [16], ethers [17] and fluorenes [18]. In the present work we report the effect of β-CDx on the excited state properties of 6-aminobenzothiazole.

Experimental

Materials

6ABT was obtained from Aldrich and purified by recrystallisation from aqueous ethanol. β-cyclodextrin was purchased from s.d. fine chemicals and used as received. Triple distilled water was used for the preparation of experimental solutions. A modified Hammett acidity scale (H_0) was employed for the solutions below pH 1.5 (using a H_2SO_4-H_2O mixture). The concentration of the experimental solution was 1.04×10^{-4} moldm^{-3}. Solutions for absorptiometric and fluorimetric titrations were prepared just before taking measurements. The isosbestic wavelengths were used for measuring the fluorescence intensities at any analytical wavelength.

Instruments

Absorption spectra were recorded with HITACHI model U-2001 spectrophotometer while fluorescence measurements were made using a Shimadzu RF-5301 PC spectrofluorometer. pH values in the range of 1–12 were measured using an ELICO LI-10T model pH meter. Fluorescence lifetimes were determined using a time-correlated picosecond photon counting spectrofluorometer (Tsunami, Spectraphysics, USA). FT-IR spectra were obtained with Avatar-330 FT-IR spectrophotometer using KBr pellet. The range of spectra was from 500–4000 cm^{-1}. Microscopic morphological structure measurements were performed with JEOI-JSM 5610LV scanning electron microscope (SEM).

Job's Continuous Variation Method

Equimolar solutions of the guests and the corresponding β-CDx were prepared and mixed to standard volumes and proportions in order that the total concentration remained constant ($[G]_t+[\beta\text{-CDx}]_t=M$) but the ratio of the initial concentrations varied between 0 and 1. ΔOD values in the preparations of guests were calculated by measuring the absorbance of guest in the absence (A_0) and the presence (A) of the corresponding concentrations of β-CDx. Also, an equimolar solution of β-CDx was used as a blank, to take into account of refractive index.

Preparation of Solid Complexes

Solid 6ABT-β-CDx complex was prepared using co-precipitation method. 6ABT and β-CDx with 1:1 molar ratio were accurately weighed. Saturated β-CDx solution was prepared in water. Then, 6ABT solution in methanol

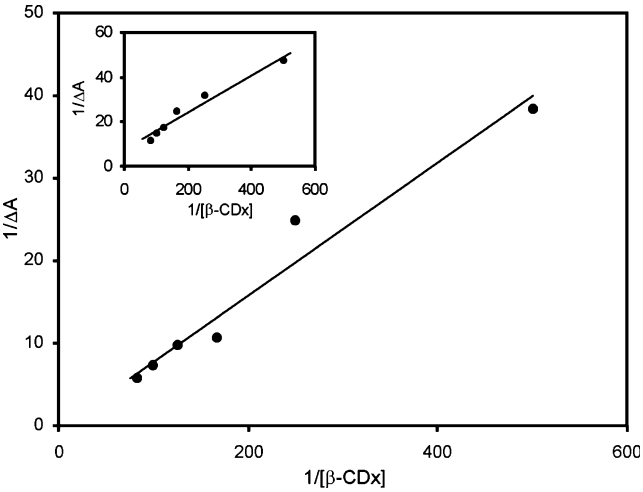

Fig. 1 Double reciprocal absorption plot of 6ABT with β-CDx at pH-6.9 [Inset : Double reciprocal absorption plot of 6ABT with β-CDx at pH-1.1]

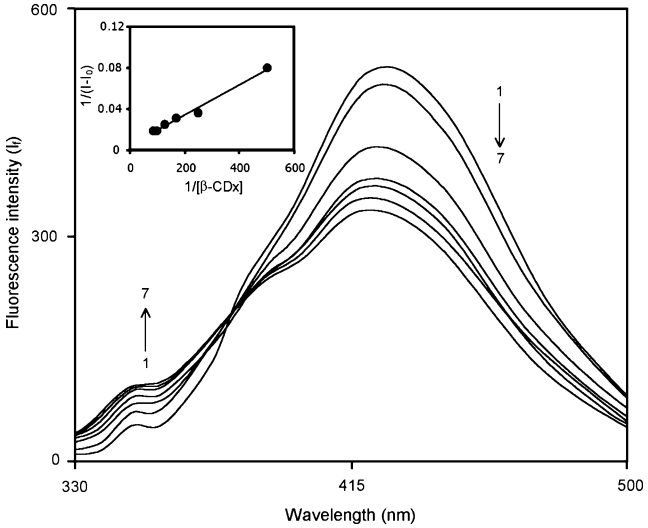

Fig. 2 Emission spectra of 6ABT with increasing concentrations of β-CDx at pH-6.9 [1.without β-CDx, 2. 0.002 M, 3. 0.004 M, 4. 0.006 M, 5. 0.008 M, 6. 0.010 M and 0.012 M β-CDx]. (Inset: Double reciprocal emission plot of 6ABT with β-CDx at pH-6.9)

was added slowly and a suspension was formed. The suspension was stirred at 40°C for 30 min and kept stirring at room temperature for 24 h. The precipitate obtained was filtered through 0.45 μm membrane filter and dried at 110°C in an oven for 2 h. The dried complex was ground to a fine powder.

Results and Discussion

The absorption maxima, absorbance and fluorescence maxima of 6ABT at different concentrations of β-CDx at pH 6.9 and pH 1.1 are given in Table 1. 6ABT exists as neutral form at pH 6.9 and monocation at pH 1.1.

Upon increasing the concentration of β-CDx, the absorption maxima were slightly blue shifted with a gradual increase in absorbance of 6ABT at both pH. The absorbance of each form increases with increasing concentrations of β-CDx upto 1.2×10^{-2} M. At higher concentrations of β-CDx, the absorption maxima and absorbance remain unchanged.

The absorption maxima and absorbance of 6ABT with different concentrations of β-CDx at pH 1.1 are significantly different when compared with the same solutions at pH 6.9. But no significant change was observed in the absorption spectra of 6ABT with different concentrations of β-CDx at pH above 7.0. An increase in the absorbance with

Table 2 Fluorescence lifetime and amplitudes of 6ABT with increasing concentrations of β-CDx (Excitation wavelength= 310.0 nm, detection wavelength = 349.0 nm)

Concentrations of β-CDx (M)	Lifetime (Sec)	Relative amplitude	χ^2	Standard deviation
0	6.52×10^{-10}	100	1.099	3.244×10^{-12}
0.002	6.16×10^{-10}, 1.98×10^{-9}	42.94, 57.06	1.17	4.21×10^{-11}, 1.68×10^{-11}
0.004	6.05×10^{-10}, 1.38×10^{-9}	10.43, 89.57	0.92	1.16×10^{-11}, 6.38×10^{-11}
0.006	5.82×10^{-10}, 1.67×10^{-9}	7.99, 92.01	1.20	3.16×10^{-11}, 7.04×10^{-11}
0.008	5.60×10^{-10}, 2.45×10^{-9}	5.81, 94.19	1.35	6.15×10^{-12}, 4.10×10^{-12}
0.010	5.39×10^{-10}, 2.99×10^{-9}	4.87, 95.13	1.18	6.03×10^{-12}, 1.54×10^{-10}
0.012	5.28×10^{-10}, 3.35×10^{-9}	1.88, 98.12	1.22	9.44×10^{-12}, 4.08×10^{-11}

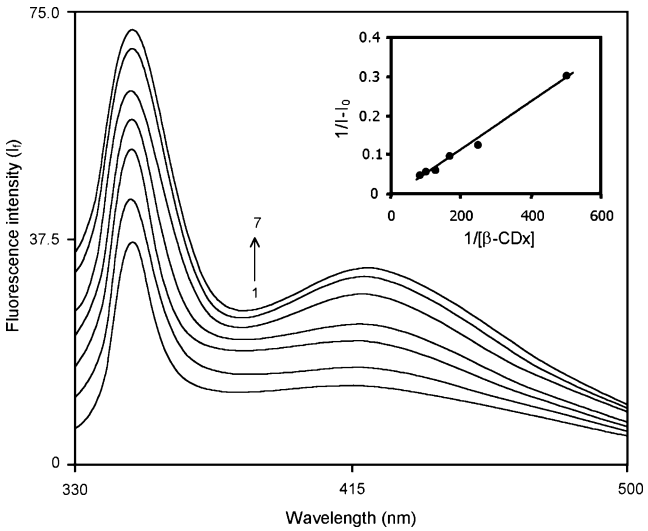

Fig. 3 Emission spectra of 6ABT with increasing concentrations of β-CDx at pH-1.2 [1.without β-CDx, 2. 0.002 M, 3. 0.004 M, 4. 0.006 M, 5. 0.008 M, 6. 0.010 M and 0.012 M β-CDx]. (Inset: Double reciprocal emission plot of 6ABT with β-CDx at pH-1.1)

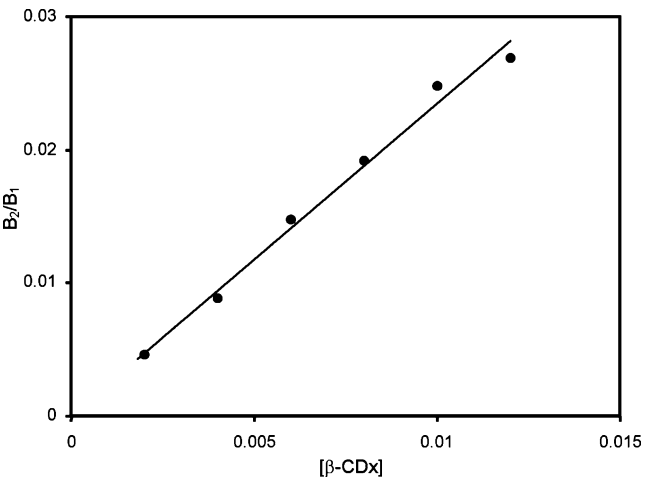

Fig. 4 Plot of B_2/B_1 Vs [β-CDx]

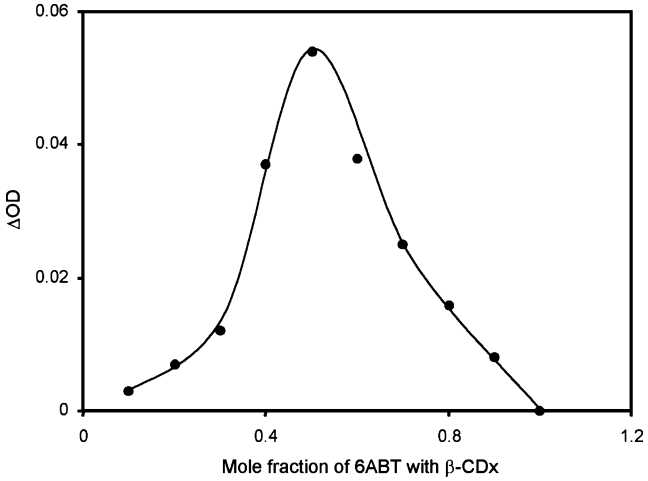

Fig. 5 Job's plot of 6ABT with β-CDx

the blue shifted maxima of the guest molecule while increasing the concentrations of β-CDx during the formation of an inclusion complex between guest and β-CDx has been reported [19].

The stoichiometry and the binding constant of the inclusion complex of neutral and monocationic forms of 6ABT with β-CDx can be determined from the changes in absorbance of 6ABT by the addition of β-CDx using Benesi-Hildebrand (BH) equation [20, 21]. The BH equation for 1:1 complex is given below.

$$\frac{1}{\Delta A} = \frac{1}{\Delta\varepsilon[6ABT]} + \frac{1}{K[6ABT]_o \Delta\varepsilon[\beta - CDx]_o} \quad (1)$$

where, ΔA is the difference between the absorbance of 6ABT in the presence and absence of β-CDx, Δε is the difference between molar absorption co-efficients of 6ABT in the presence and absence of β-CDx, $[6ABT]_o$ and $[\beta\text{-CDx}]_o$ are the initial concentrations of 6ABT and β-CDx, respectively and K is the binding constant.

Figure 1 gives the double reciprocal plots, between 1/(ΔA) and $\frac{1}{[\beta-CDx]}$ for neutral and monocationic forms of 6ABT with β-CDx. The linearity of the plots shows the stoichiometric ratio of the complex of neutral and monocationic forms of 6ABT with β-CDx is 1:1. Therefore each form of 6ABT can be accommodated with one molecule of β-CDx. From the slope of the straight line, the binding constants (K) were calculated as 71.4 and 109.75 m^{-1} for neutral and monocationic forms of 6ABT, respectively at 303 K.

Figures 2 and 3 shows the fluorescence emission spectra of 6ABT at pH 6.9 and 1.1 with increasing concentrations of β-CDx, respectively. In aqueous media, there are two maxima at 349.0 and 426.0 nm for 6ABT at both pH. At pH 6.9, by the addition of β-CDx, the fluorescence intensity at longer wavelength (426.0 nm) is decreased with an increase in the fluorescence intensity at shorter wavelength (349.0 nm). The fluorescence intensity at longer wavelength is significantly higher than at shorter wavelength. The reason is a explained as follows. 6ABT exist as neutral form at pH 6.9. So the lone pair of electrons on nitrogen interacts with –OH groups of β-CDx via the hydrogen bonding interaction. Further addition of β-CDx increases the hydrogen bonding interactions to a greater extent. Hence the fluorescence intensity of 6ABT at longer wavelength is decreased whereas the fluorescence intensity at shorter wavelength is increased. But at pH 1.1, the fluorescence intensity increases at both wavelengths (Fig. 3). Here, the hydrogen bonding interaction between lone pair of electrons on N-atom of $–NH_2$ group and –OH group of β-CDx is arrested due to formation of monocation at pH 1.1 by the protonation of amino group.

No significant change in the fluorescence intensity was observed by the further addition of β-CDx at both pH. This shows that the complexation is complete at 1.2×10^{-2} M β-CDx.

The β-CDx dependence of 6ABT fluorescence intensity is analysed by the BH equation for 1:1 complex.

$$\frac{1}{(I - I_0)} = \frac{1}{(I' - I_0)} + \frac{1}{K[I' - I_0][\beta - CDx]} \quad (2)$$

where K is the binding constant, I_0 is the intensity of fluorescence of 6ABT without β-CDx, I is the fluorescence intensity at certain concentration of β-CDx and I′ is the fluorescence intensity with the highest concentration of β-CDx.

The double reciprocal plot of $\frac{1}{(I-I_0)}$ *Vs* $\frac{1}{(\beta-CDx)}$ is given in inset of Figs. 2 and 3 for neutral and monocationic forms of 6ABT, respectively. From the linearity of the plots, the stoichiometric ratio of the inclusion complex of 6ABT and its monocation with β-CDx is found to be 1:1. From the slope of the straight line, the binding constants were calculated to be 68.43 and 86.95 M^{-1} at

Table 3 Binding constant and Gibb's free energy change values of 6ABT in β-CDx medium

Parameters	pH 6.9		pH 1.2	
	λ_{abs}	λ_{flu}	λ_{abs}	λ_{flu}
K (M^{-1})	71.40	68.43	109.75	86.95
ΔG ($kJmol^{-1}$)	−10.132	−10.012	−13.117	−11.741
Regression coefficient, r	0.9783	0.9931	0.9794	0.9957
Standard deviation	2.988	0.00304	3.0212	0.01065

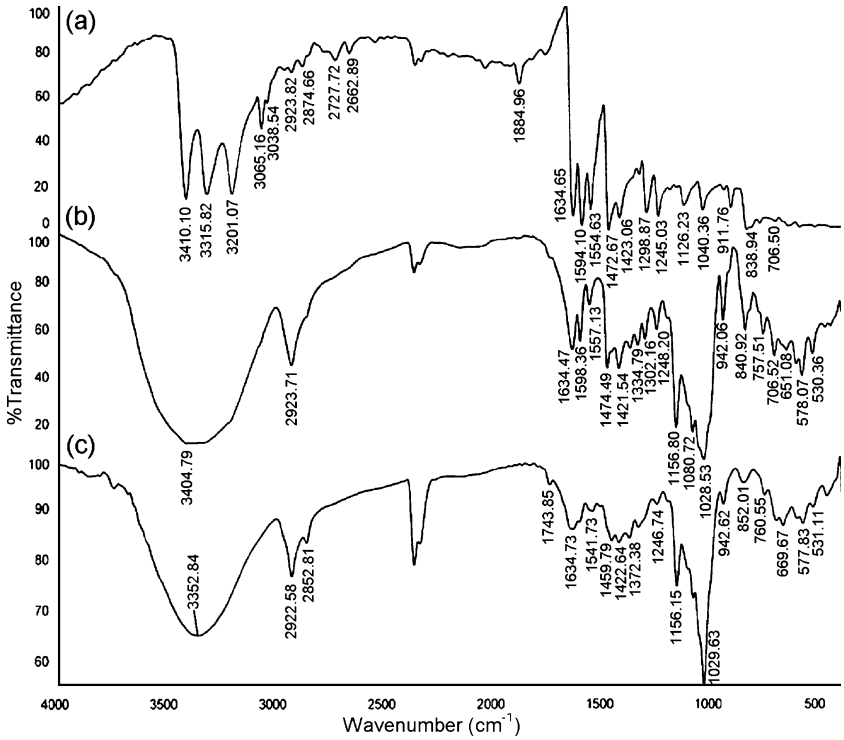

Fig. 6 FT-IR spectra of **a** Pure 6ABT, **b** Physical mixture of 6ABT with β-CDx and **c** Solid inclusion complex of 6ABT with β-CDx

pH 6.9 and pH 1.1, respectively. The binding constants obtained from absorption and fluorescence data are close to each other.

The formation of the inclusion complex was also confirmed by the fluorescence decay curves for 6ABT with different concentrations of β-CDx. The lifetimes and their amplitudes of 6ABT with and without β-CDx are given in Table 2. The time-resolved fluorescence of 6ABT with β-CDx shows bi-exponential decay indicating the equilibrium between free and complexed forms and the amplitude increases with the increasing concentrations of β-CDx upto 12×10^{-3} M. Above 12×10^{-3} M, no change was observed in lifetime and amplitude of 6ABT. The x^2 values for the single and bi-exponential fittings are less than 1.37.

The ratio of the pre-exponential factors (B_2/B_1) is related to the concentration of the two components by the equation (3) [22].

$$\frac{B_2}{B_1} = C_2 \mathrm{kr}_2 \varepsilon_2 / C_1 \mathrm{kr}_1 \varepsilon_1 \tag{3}$$

where C, kr and ε are the concentration of 6ABT, the radiative rate constant and the molar absorption co-efficient at the excitation wavelength, respectively. The subscripts 1 and 2 refer the free and complexed 6ABT with β-CDx, respectively. Since kr is a constant and $\varepsilon_1=\varepsilon_2$, Eq. 3 is simplified as $B_2/B_1 \approx C_2/C_1$. In excess of [β-CDx] with respect to the 6ABT, B_2/B_1 can be written as Eq. 4.

$$\frac{B_2}{B_1} = \mathrm{K}[\beta - \mathrm{CDx}] \tag{4}$$

The plot of B_2/B_1 *Vs* [β-CDx] is given in Fig. 4. The linearity of the plot reveals the formation of 1:1 complex between 6ABT and β-CDx. From the slope of the straight line, binding constant 'K' was calculated to be 70.42 M^{-1}.

The stoichiometry of the inclusion complex between 6ABT and β-CDx was also confirmed by the plots of Job's continuous variation method using absorption spectral data. Figure 5 represents the change in optical density (ΔOD) against the molefraction of 6ABT. In this plot ΔOD is maximum at 0.5 indicating the stoichiometry of the complex between 6ABT and β-CDx is 1:1.

The free energy change (ΔG) of this inclusion complex formation was determined from the binding constant at 303 K using the following equation.

$$\Delta \mathrm{G} = -\mathrm{RTlnk} \tag{5}$$

The negative values of ΔG (Table 3) indicate that the formation of inclusion complex between 6ABT and β-CDx is exergonic and spontaneous process at 303 K.

With aqueous D(+)-glucose, the absorption and fluorescence spectra of 6ABT are not significantly changed, which confirms that all the spectral changes in β-CDx are due to

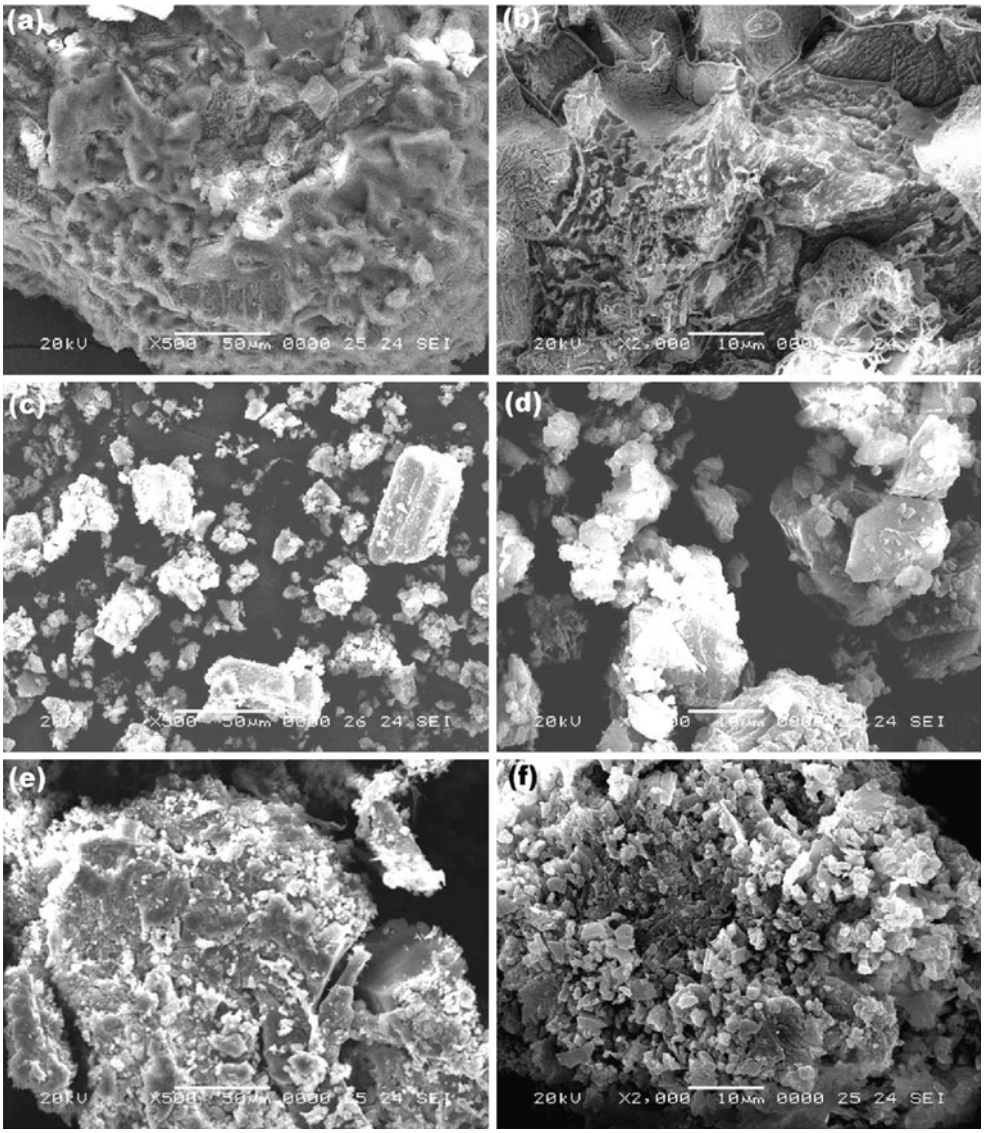

Fig. 7 SEM images of **a** Pure 6ABT (×500), **b** Pure 6ABT (×2000), **c** Physical mixture of 6ABT with β-CDx (×500), **d** Physical mixture of 6ABT with β-CDx (×2000), **e** Solid inclusion complex of 6ABT with β-CDx (×500) and **f** Solid inclusion complex of 6ABT with β-CDx (×2000)

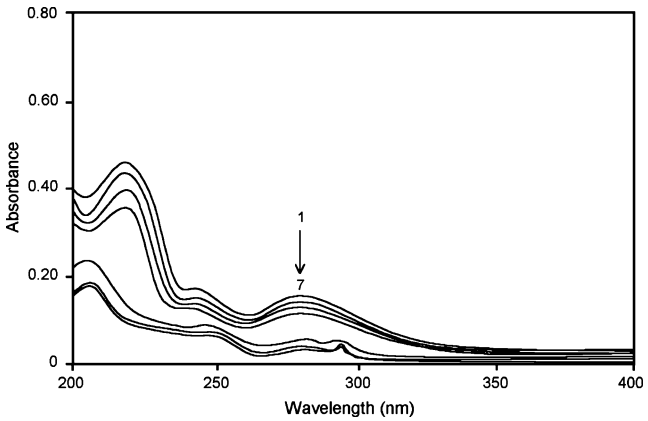

Fig. 8 Absorption spectra of 6ABT without β-CDx at different pH values (1. pH 6.8, 2. pH 5.8, 3. pH 5.0, 4. pH 4.2, 5. pH 3.0, 6. pH 2.0, 7. pH 1.1)

inclusion complexation and not due to any non-inclusion complex formation.

A solid state complex was prepared by co-precipitation method and characterized by FT-IR spectral and SEM

Table 4 Absorption and fluorescence spectral maxima of neutral and monocationic forms of 6ABT in aqueous and β-CDx media

pH	Absorption maxima (nm)		Fluorescence maxima (nm)	
	Aqueous medium	β-CDx medium	Aqueous medium	β-CDx medium
7.0	282.0 244.2 223.8	280.2 242.2 225.2	349.0 426.0	348.0 420.0
1.2	291.0 (s) 241.4	288.6 281.2 240.2	–	–

s-shoulder

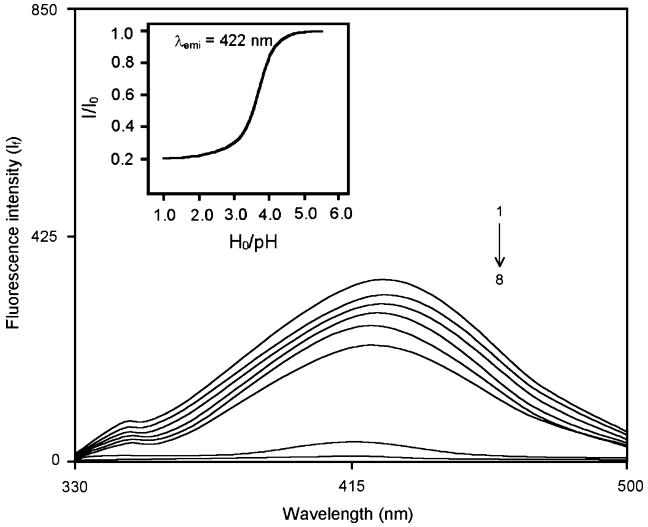

Fig. 9 Emission spectra of 6ABT without β-CDx at different pH values (1. pH 8.4, 2. pH 6.8, 3. pH 5.8, 4. pH 5.0, 5. pH 4.2, 6. pH 3.0, 7. pH 2.0, 8. pH 1.1, λ_{exc}=317.9 nm) (Inset: Fluorimetric titration curves of 6ABT without β-CDx medium)

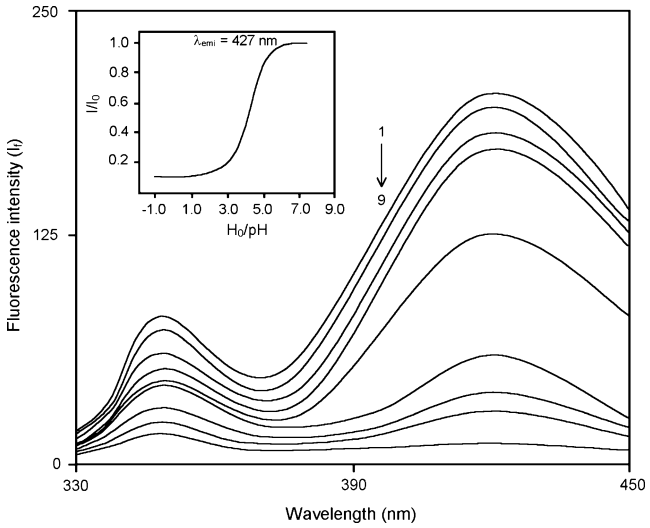

Fig. 11 Emission spectra of 6ABT with β-CDx at different pH values (1. pH 7.5, 2. pH 6.7, 3. pH 5.2, 4. pH 4.1, 5. pH 3.1, 6. pH 2.3, 7. pH 1.7, 8. pH 1.1, 9. pH 0.26, λ_{exc}=318.0 nm) (Inset: Fluorimetric titration curves of 6ABT with β-CDx medium)

image. The FT-IR spectra of pure 6ABT, physical mixture of 6ABT and β-CDx and solid complex of 6ABT with β-CDx are shown in Fig. 6. The N-H stretching frequency of pure 6ABT appeared at 3410.10 cm^{-1}, is significantly shifted to 3352.84 cm^{-1} in the case of solid complex. In the physical mixture the N-H stretching frequency of pure 6ABT appeared at 3404.8 cm^{-1}. The C-H aromatic stretching frequency appeared at 3065 cm^{-1} is not observed in solid complex. The C-S stretching frequency of pure 6ABT appeared at 706.5 cm^{-1} is shifted to 760 cm^{-1} in solid complex. Further, the absorption intensities of most of the stretching frequencies in the solid complex are significantly weaker (10–20%) than for pure 6ABT.

The SEM images of powdered form of 6ABT, physical mixture of 6ABT with β-CDx and the solid inclusion complex are shown in Fig. 7. The different morphologies observed support the formation of inclusion complex. The physical mixture of 6ABT and β-CDx powders revealed the similarities with the crystals of the free molecules of 6ABT and β-CDx.

Overall, the FT-IR spectral and SEM image analysis indicate the formation of inclusion complex between 6ABT and β-CDx and also demonstrate that no complex is formed in the physical mixture of the compounds.

The effect of pH on the absorption spectra of 6ABT without β-CDx is shown in Fig. 8 and the relevant spectral data is given in Table 4. With the decrease of pH from 6, the absorption maxima of the neutral form obtained at 282.0 and 244.2 nm are blue shifted continuously and becomes constant at pH 1.2. The blue shifted spectrum observed with the maximum at 241.4 nm is due to the protonation of $-NH_2$ group of 6ABT. The ground state acidity constant (pK_a) of the monocation-neutral equilibrium is determined spectrophotometrically to be 3.9.

The fluorescence emission spectra of 6ABT without β-CDx at various H_0/pH values are shown in Fig. 9. The spectrum with the maxima at 349.0 and 426.0 nm corresponds to the neutral form of 6ABT. Above pH 8.4 there is no change in the fluorescence maxima and its intensity.

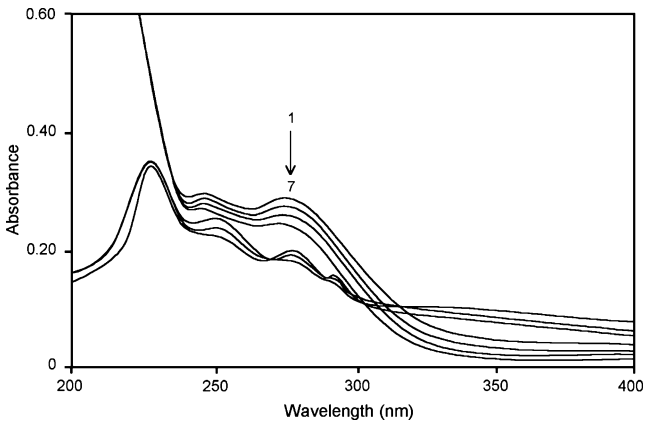

Fig. 10 Absorption spectra of 6ABT with β-CDx at different pH values (1. pH 6.7, 2. pH 5.2, 3. pH 4.1, 4. pH 3.1, 5. pH 2.3, 6. pH 1.7, 7. pH 1.2)

Table 5 The ground and excited state acidity constant values of 6ABT in aqueous and β-CDx media

Equilibrium monocation ⇋ neutral	Ground state pK_a	Excited state pK_a
Without β-CDx	3.9	3.8
With β-CDx	3.2	3.1

Table 6 Bond lengths between various atoms of 6ABT and its cation

Atoms	Bond distance (Å)
Neutral	
C_1–C_8	3.58
C_1–H_{14}	4.57
H_{15}–S_9	6.04
H_{16}–S_9	5.32
H_{11}–H_{12}	5.04
Cation	
C_1–C_8	3.58
C_1–H_{14}	4.57
H_{15}–S_9	6.01
H_{16}–S_9	5.29
H_{17}–S_9	5.66
H_{11}–H_{12}	5.06

Decrease of pH from 5.0, causes a decrease in the fluorescence intensity of both maxima upto pH-1.5. No fluorescence was observed at below pH-1.5. This shows the non-fluorescent nature of monocation obtained by the protonation of amino group. In this case the pK_a* value for monocation-neutral equilibrium is obtained from the quenching curve of the neutral form (Inset Fig. 9).

The absorption spectra of 6ABT in β-CDx at various pH values are shown in Fig. 10. With decrease of pH from 5.0, the absorption maxima at 280.2, 242.2 and 225.2 nm corresponding to the neutral form of 6ABT are red shifted. The absorption spectrum with the maxima at 288.6, 281.2 and 240.2 nm corresponds to the monocation of 6ABT formed by the protonation of amino group. The reason for observing red shift instead of blue shift, during the formation of monocation of 6ABT is due to decrease in the interaction between the lone pair of electrons of amino group of 6ABT and OH groups of β-CDx. The ground state pK_a value for the neutral-monocation equilibrium of 6ABT in β-CDx is found to be 3.2. This value is less than the pK_a value of 3.9 in aqueous solution.

The fluorescence spectra of 6ABT in β-CDx at various H_0/pH values are shown in Fig. 11. With decrease of pH from 6.0, there is a decrease in the intensity of fluorescence of the neutral form at 348.0 and 420.0 nm upto pH 0.26. Below this, no fluorescence was observed. This shows that the monocation is non-fluorescent. The pK_a* obtained from the quenching curve of the neutral form is found to be 3.1. The ground and excited state acidity constant values of 6ABT in aqueous and β-CDx media are given in Table 5.

Calculations using the software-MOPAC/AM1 show that length of 6ABT molecule and its cation $6ABTH^{\oplus}$ is 6.04 and 6.01 Å, respectively (Table 6). The diameter of β-CDx cavity is 7.8 Å. Hence, there is a possibility of complete accommodation of whole molecule of 6ABT and its cation within the cavity of β-CDx. But based on low values of binding constant, the structures of inclusion complexes of 6ABT and its cation in β-CDx are proposed as in Fig. 12.

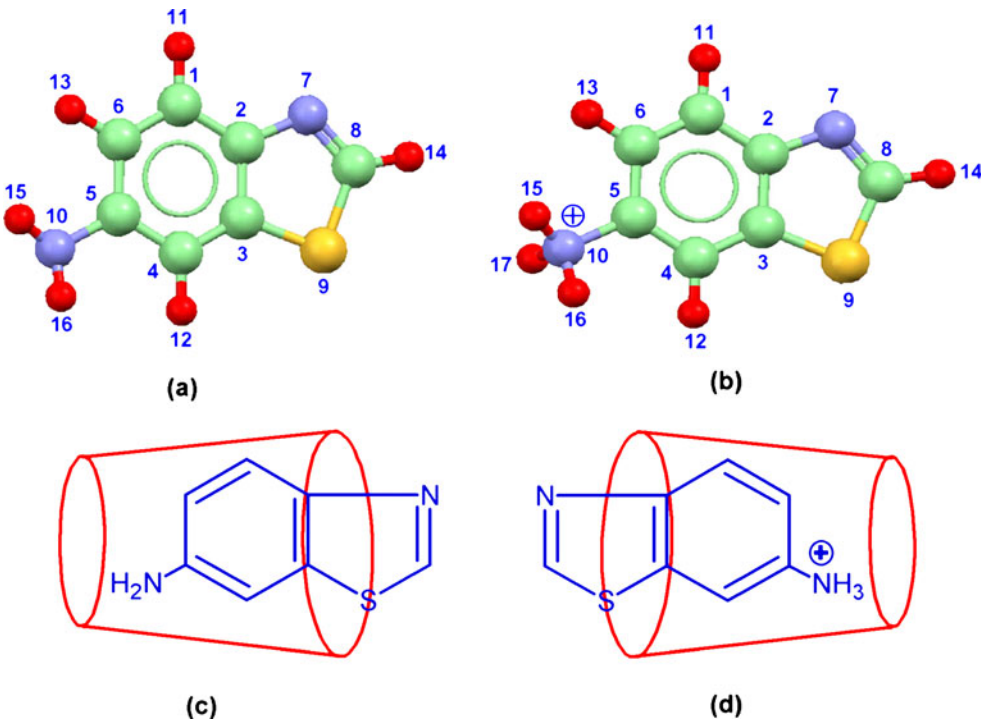

Fig. 12 MOPAC/AM1 of **a** optimized structure of 6ABT, **b** optimized structure of $6ABTH^{\oplus}$, **c** schematic diagram of inclusion complex (1:1) of 6ABT with β-CDx and **d** schematic diagram of inclusion complex (1:1) of $6ABTH^{\oplus}$ with β-CDx

Conclusions

The following conclusions can be made based on the results. (i) From the Benesi-Hildebrand plot it has been found that the stoichiometry of the complex of neutral and monocationic forms of 6ABT with β-CDx is 1:1. (ii) The lone pair of electron in amino group of nitrogen plays an important role in the excited state of 6ABT to form the inclusion complex with β-CDx. (iii) Bi-exponential decay shows presence of the two species of 6ABT namely free and complex forms with β-CDx. (iv) FT-IR spectral and SEM image analysis of solid complex confirms the formation of inclusion complex between 6ABT and β-CDx. (v) There is significant difference in ground and excited state acidity constant of 6ABT in aqueous and β-CDx media. Based on the results, the structure of the 1:1 complex between 6ABT and β-CDx is proposed.

Acknowledgement We are grateful thank to The National Centre for Ultrafast Processes (NCUFP), University of Madras, Chennai, for fluorescence lifetime measurements.

References

1. Szejtli J (1982) Cyclodextrin and their inclusion complexes. Akademic Kiado, Budapest
2. Szejtli J, Osa T (1996) Comprehensive supramolecular chemistry, Elsevier Science Ltd., Oxford (U.K.)
3. Duchene D (1988) Cyclodextrins and their industrial uses. Editions de Sante, Paris
4. Scypinski S, Love C (1984) Cyclodextrin-induced room temperature phosphorescence of nitrogen heterocycles and bridged biphenyls. Anal Chem 56:331–336
5. Sano A, Takezawa M, Takitani S (1989) Spectrofluorimetric determination of cynide in blood and urine with naphthalene-2, 3-dialdehyde and taurine. Anal Chim Acta 225:351–358
6. Munoz Dalapena A, Ndou TT, Zung JB, Greene KL, Live DH, Warner IM (1991) Alcohol size as a factor in the ternary complex formed with pyrene and β-cyclodextrin. J Am Chem Soc 113:1572–1577
7. Ramamurthy V, Eaten DF (1988) Photochemistry and photophysics with cyclodextrin cavities. Acc Chem Res 21:300–306
8. Ramamurthy V, Weiss RG, Hammond G (1993) A model for the influence of organized media on photochemical reaction. Adv Photochem 18:67–234
9. Kalyanasundaram K (1987) Photochemistry in microheterogenous systems. Academic, New York
10. Kleinman MH, Bohne C (1997) Organic photochemistry: Molecular and supramolecular photochemistry. Marcel Dekkar Inc, New York
11. Bortolus P, Monti S (1996) Photochemistry in cyclodextrin cavities. Adv Photochem 21:1–133
12. Bender ML, Komiyama A (1978) Cyclodextrin chemistry. Springer Verlag, New York, pp 23–30
13. Connors KA (1997) The stability of cyclodextrin complexes in solution. Chem Rev 97:1325–1358
14. Ibrahim AMA (1993) Charge transfer complexes of Schiff bases derived from 2-aminobenzothiazole with some acidic and non-acidic acceptors. Can J Chem 71:318–324
15. Rajamohan R, Kothai Nayaki S, Swaminathan M (2008) Spectrofluorimetric study on inclusion complexation and photoprototropic behaviour of 2-amino-6-fluorobenzothiazole with β-cyclodextrin. Coll Czech Chem Comm 73(2):147–160
16. Rajamohan R, Kothai Nayaki S, Swaminathan M (2007) Inclusion complexation and photoprototropic behaviour of 3-amino-5-nitrobenzisothiazole with β-cyclodextrin. Spectrochim Acta A 69:371–377
17. Muthu Vijan Enoch IV, Swaminathan M (2007) Fluorimetric and prototropic studies on the inclusion complexion of 2-amino and 4-aminodiphenyl ethers with β-cyclodextrin: Unusual behaviour of 4-aminodiphenyl ether. J Lumin 127:713–720
18. Muthu Vijan Enoch IV, Swaminathan M (2006) Fluorimetric study on molecular recognition of β-cyclodextrin and 2-amino-9-fluorenone. J Fluores 16:501–510
19. Hoshino M, Imamura M, Ikehara K, Hama Y (1981) Fluorescence enhancement of benzene derivatives by forming inclusion complexes with β-cyclodextrin in aqueous solution. J Phys Chem 85:1820–1823
20. Cho DW, Kim YH, Kang SG, Yoon M, Kim D (1996) Cyclodextrin effects on intramolecular charge transfer of 2-biphenylcarboxylic acid: a pre-twisted molecule. J Chem Soc Faraday Trans 92:29–34
21. Benesi HA, Hildebrand JH (1949) A spectroscopic investigation of the interaction of iodine with aromatic hydrocarbons. J Am Chem Soc 71:2703–2707
22. Monti S, Kohler G, Grabner G (1993) Photophysics and photochemistry of methylated phenols in β-cyclodextrin inclusion complexes. J Phys Chem 97:13011–13016